Excitation dynamics in $La_{0.875}Sr_{0.125}MnO_3$ measured by resonant Auger electron and resonant x-ray emission spectroscopies

T. O. Menteş,[1] F. Bondino,[2] E. Magnano,[2] M. Zangrando,[2] K. Kuepper,[3,4] V. R. Galakhov,[5] Y. M. Mukovskii,[6] M. Neumann,[4] and F. Parmigiani[1,2,7]

[1]*Sincrotrone Trieste Area Science Park, Basovizza-Trieste, Italy*

[2]*Laboratorio Nazionale TASC INFM-CNR, Basovizza-Trieste, Italy*

[3]*Forschungszentrum Rossendorf, Institute of Ion-Beam Physics and Materials Research, Bautzner Landstrasse 128, D-01328 Dresden, Germany*

[4]*University of Osnabrück, Department of Physics, Barbarastrasse 7, D-49069 Osnabrück, Germany*

[5]*Institute of Metal Physics, Russian Academy of Sciences - Ural Division, 620219 Yekaterinburg GSP-170, Russia*

[6]*Moscow State Steel and Alloys Institute, 119049 Moscow, Russia*

[7]*Dipartimento di Fisica, Università degli Studi di Trieste, Trieste, Italy*

(Received 20 April 2006; published 6 November 2006)

The charge transfer dynamics of an underdoped manganite is probed by resonant x-ray emission and Auger electron spectroscopies at the Mn L_3 edge. The dispersion of peak positions, as the incident photon energy is tuned through the absorption threshold, gives direct information on the relaxation rate in terms of the core-hole lifetime and the localization behavior of the states involved. The charge transfer time is found to be around 0.45 fs, with a dependency on the final state *d*-band occupancy.

DOI: 10.1103/PhysRevB.74.205409 PACS number(s): 79.60.−i, 72.15.Lh, 71.70.Ch, 78.70.En

I. INTRODUCTION

The manganites are complex compounds which have been a subject of much interest in the last decade owing to their properties potentially useful for technological applications and to their analogy to high-T_c superconductors. The competition between the spin, charge, orbital, and lattice degrees of freedom provides a rich variety of phases.[1,2] Fundamentally, regardless of the details of the particular theory, the coupling between the Mn and O atoms is very important, as oxygen is the mediator of the indirect exchange interactions between the Mn atoms. As shown in various studies, the bonding between manganese and oxygen has a partial covalent character,[3] influencing both the magnetic and transport properties. Therefore, it is of interest to investigate the electronic structure of Mn emphasizing the Mn-O charge transfer.

In the present study, we will demonstrate the use of resonant x-ray spectroscopies in understanding the charge-transfer dynamics in a three-dimensional manganite $La_{0.875}Sr_{0.125}MnO_3$. At this particular Sr concentration, one finds orbital and charge ordering, and a very unusual ferromagnetic insulating phase, which are discussed in the literature.[4–6] These phenomena cannot be explained through simple models such as double exchange,[7] making $La_{0.875}Sr_{0.125}MnO_3$ a key compound for a better understanding of the colossal magneto-resistance effect.

For a system in a core level excited state, the competition between the charge transfer and core-hole decay processes manifests itself as a correlation (or its absence) between the excitation and deexcitation channels.[8] This competition is used to obtain information on the charge-transfer dynamics within the time scale corresponding to the core-hole decay, providing an alternative technique to pump-probe measurements.[9] In terms of the particular technique used, resonant Auger electron spectroscopy (RAES) has proved to be a valuable tool, especially obvious in measurements involving weakly coupled adsorbate-substrate interactions (see, for example, Ref. 10). Though less commonly used, resonant x-ray emission (RXES) bears the same principles of interest, and will be utilized in the following as a complementary technique to RAES.

Dominantly the Auger electron and to a lesser extent x-ray emission constitute the majority of the decay channels for an ion excited above its ground state in the soft x-ray regime. The incoming photon creates a core-hole, which is subsequently filled by an electron coming from a shallower core level or the valence band. The energy released either kicks out an electron from the ion (radiationless decay, Auger electron emission) or is emitted as a photon (radiative decay, x-ray emission). In the nonresonant case, where the incident photon energy is far above the absorption threshold of the core level of interest, the excitation and deexcitation steps can be viewed as being independent. The photoemitted electron is not involved in the relaxation of the intermediate state nor in the deexcitation of the ion. The outgoing Auger electron has a specific kinetic energy, which is determined by the energy difference between the intermediate state (singly charged) and the final state (doubly or singly charged for Auger electron or x-ray emission) independent of the incident photon energy. On the other hand, when the photon energy is tuned close to the absorption threshold, the photo excited electron has just enough energy to reach the empty states in the valence band. Therefore, there is a chance that it will participate in the deexcitation. In this case, the energy of the Auger electron (or the emitted photon in RXES) depends on the incident photon energy. The resulting behavior, with the clear signature in the dispersion of the peak positions, is termed as Raman-Auger emission or Raman scattering. Increasing the photon energy further, the excited electron will finally be able to "escape" before the ion can decay. This transition is viewed as a change from a one-step (coherent) to a two-step (incoherent) process.

The existence of Raman behavior around the absorption edge, and its evolution to the nonresonant process with increasing photon energy, depend on the relaxation dynamics in the intermediate state. The transition between the two regimes is governed by the competition between the time scales corresponding to the core-hole decay and the charge transfer (or in more general terms, the delocalization of the excited core electron in the intermediate state). The intensity ratio between the coherent and incoherent channels in the scattering will be proportional to the ratio of the two competing rates, under the assumption that both the core-hole decay and the charge transfer have exponential time dependences. Most of the quantitative studies of "femtosecond" RAES up to date have used this idea in cases where the two channels could be distinguished through a shift in energy or by means of a complementary measurement on a similar but isolated ion.[8] However, a crucial ingredient, which has to be taken into account, is the fact that the considered rates are not simply constants, but they change throughout the absorption threshold. We will demonstrate in the following sections that this fact is closely related to the transition from Raman to normal emission behavior for a particular spectral feature. As was suggested by earlier measurements (e.g., Ref. 10), the charge transfer time may possibly depend on the intermediate state. This is due to the excitations into orbitals hybridized with the neighboring atoms, which have higher probability of delocalizing in a given time. On the other hand, close to the threshold, the core-hole decay time has to be replaced by an "effective scattering time," which depends on the photon energy relative to the absorption edge.[11,12]

The last statement can be extracted from the resonant scattering amplitude, described in the Kramers-Heisenberg formulation,[8,11] as it will be shown in the following. If we consider the excitation by an incoming photon of energy E_γ of an atom from its ground state $|0\rangle$ to all possible intermediate levels $|j\rangle$ of energies E_{j0} and the subsequent decay to a final state $|f\rangle$, the resonant scattering amplitude is given by[8,11]

$$F_{\text{resonant}} = \sum_j \frac{\langle f|Q|j\rangle\langle j|D|0\rangle}{E_\gamma - E_{j0} + i\Gamma} , \tag{1}$$

where Q and D are the Coulomb (in the Auger case) and the dipole operators, respectively, and Γ is the lifetime width of the core-hole excited intermediate state. Note that the denominator in Eq. (1) appears as an exponential considering the time dependence in the evolution of quantum states. Defining the detuning, Ω, as the energy difference $E_\gamma - E_{j0}$, one can obtain a scattering time (or effective duration of scattering), following Gel'mukhanov and Agren:[11,12]

$$\tau_c = \frac{1}{\sqrt{\Omega^2 + \Gamma^2}}, \tag{2}$$

where the contribution to resonant scattering is mostly limited to times $t < \tau_c$. It is seen that for zero detuning, namely on the resonance, the effective scattering time is given by the core-hole lifetime Γ^{-1}, whereas the scattering gets faster for larger detuning. It follows immediately that the probability of observing coherent excitation and deexcitation steps increases with detuning, purely on a quantum mechanical basis as the system will not have sufficient time for relaxation for scattering faster than the charge transfer.

The comparable core-hole decay and charge transfer times make $La_{0.875}Sr_{0.125}MnO_3$ suitable to be studied using the ideas described above, as it will be demonstrated in the following sections. The measurements were done on different decay channels following the same excitations across the Mn L_3 absorption threshold. In particular, we have measured the Mn $2p3p3d$ RAES radiationless channel and Mn $3d2p$ ($L\alpha_{1,2}$) and Mn $3s2p$ (Ll) RXES radiative decay channels as the incident photon energy was tuned through the Mn L_3 edge. The results will be interpreted in light of the similar studies on $3d$ metals and their oxides.

II. EXPERIMENTAL

Both RAES and RXES measurements were done at the elliptically polarized undulator beamline BACH at ELETTRA.[13] The incident photon energy was tuned around the Mn L edges at about 640 eV by means of a spherical grating monochromator, with a typical resolving power of about 3000. Both the inelastic scattering and the photoemission measurements were done in the same experimental chamber. The electrically isolated sample mount allowed for the absorption measurements to be carried out in the same configuration through total electron yield. The base pressure in the chamber was below 4×10^{-10} mbar during all measurements.

The x-ray spectrometer used in the RXES measurements is based on a variable-line-spacing (VLS) grating with a CCD detector placed in its focal plane.[14] The angle of the detected x-ray emission was 60° away from the direction of incidence in the horizontal plane. In order to optimize the energetic resolution and spectrometer efficiency, all the RXES data presented in this work were acquired using the second order from the VLS grating. The intensities were normalized with respect to the oxygen $1s$ emission peak, which was recorded simultaneously to the Mn $3d2p$ and $3s2p$ emission spectra. In order to collect the Auger electron emission, a 150 mm-VSW hemispherical-electron analyzer with a 16-channel detector was used.

The single crystal $La_{0.875}Sr_{0.125}MnO_3$ sample was grown by floating zone melting with radiation heating at the Moscow State Steel and Alloys Institute.[15] X-ray diffraction was used to check the structural quality and the single phase nature of the specimens. The absorption spectroscopy measurement on the sample exposed to air for long time shows a strong Mn^{2+} component, which disappears after fracturing the sample *in situ*. The clean surface was monitored by the Mn L-edge absorption spectrum, and confirmed by the absence of the 9 eV binding energy peak in the valence band photoemission spectrum, a signature of contamination.[3] All the measurements were done at room temperature in the paramagnetic-insulator state of the compound. The polarization of the incident x-ray beam was linear in the horizontal scattering plane.

III. RESONANT AUGER ELECTRON SPECTROSCOPY RESULTS

As described in the Introduction, the Mn $2p_{3/2}3p3d$ Auger electron emission can be used to study the competition be-

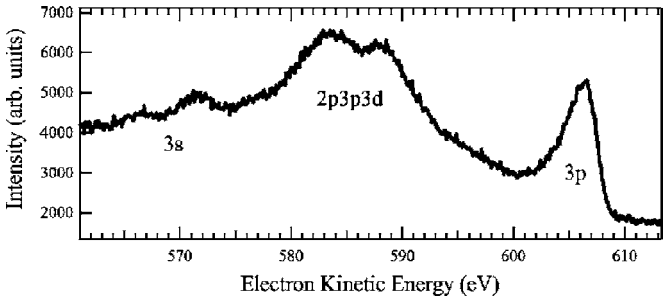

FIG. 1. The Mn3*s* and 3*p* core levels and the 2*p*3*p*3*d* Auger peaks are shown for an incident photon energy of 654 eV.

tween the charge transfer and core-hole decay, apart from the information it provides on the band structure parameters of Mn.[16] The off-resonant photoemission spectra in Fig. 1 shows several features including Mn core levels as well as the two peaks associated with the 2*p*3*p*3*d* Auger emission. The strong interaction between the final state 3*p* core hole and the *d* electrons, as well as the mixing between the oxygen *p* and the manganese *d* levels complicate the understanding of the origin of the peaks. In addition, the absence of the dipole selection rules in the deexcitation step for the nonradiative transition increases the possible number of final states greatly. With a comparison to the valence band resonant photoemission results, we assign the two peaks to different 3*d* configurations arising due to multiplet effects. The intra-

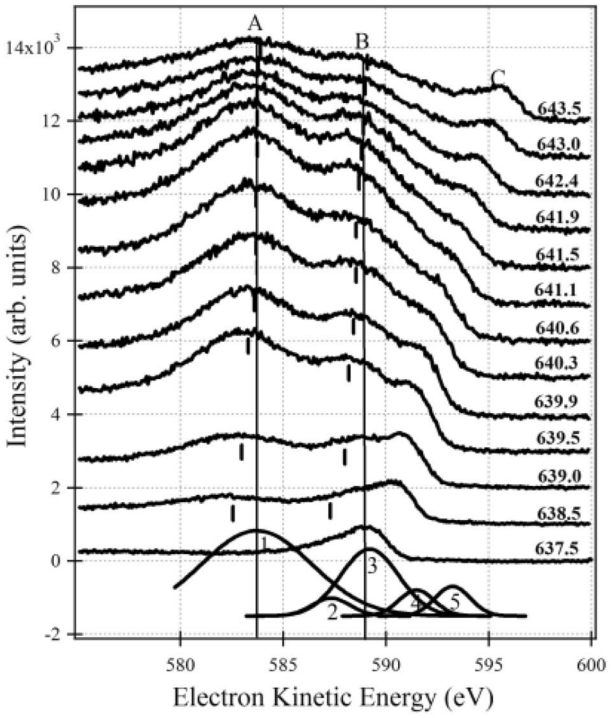

FIG. 2. Mn2*p*3*p*3*d* Auger spectra and the photoemitted 3*p* electrons as a function of photon energy. The vertical lines are drawn as a guide to the eye. The x-ray absorption spectrum (XAS) peaks at 641.3 eV. The incident photon energy for each Auger spectrum is noted on the right, and the five Gaussians used in the fit are shown for the spectrum at the XAS peak 641.3 eV.

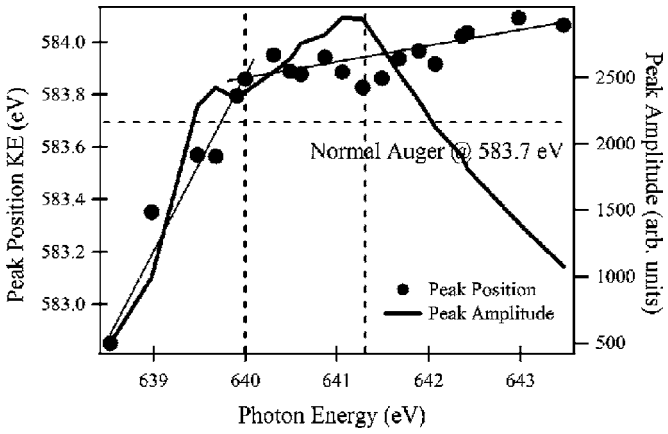

FIG. 3. Filled circles are the kinetic energy of the Auger peak *A* as a function of the incident photon energy. The solid line is the intensity of the same peak obtained from the fit as explained in the text and plotted against the photon energy. The horizontal dashed line is to mark the position of the nonresonant Auger kinetic energy of the same peak, measured 20 eV above the edge. The photon energies corresponding to the Raman-Auger to normal Auger transition, and to the XAS peak are 640.0 and 641.3 eV, respectively, as marked by vertical lines.

atomic nature of the peaks is further supported by a measurement on the gas phase Mn.[17] Regardless of the particular 3*d* configurations, the approximate values of the charge-transfer energy and the transfer integral[3,18] and the strong 3*p*-3*d* Coulomb interaction point to the possibility that there is a large charge-transfer contribution in the Auger final states.

The series of $2p_{3/2}3p3d$ Auger spectra as a function of incident photon energy are shown in Fig. 2. The objective of the data analysis was to extract the peak positions and intensities corresponding to the two main Auger components. In order to obtain a good fit to the spectra within the full range of the incident photon energies, five Gaussians were introduced in the 25 eV kinetic energy range considered.[19] The two peaks at higher kinetic energy together account for the 3*p* core level contribution, marked as *C* in the figure, where the energy difference between them was constrained to be around 1.8 eV according to a fit on the nonresonant spectra. The remaining peaks belong to the Auger components labeled as *A* (peak 1) and *B* (peaks 2 and 3). Note that the positions of peaks 2 and 3 follow a similar dispersion with an energy spacing of 2.0±0.3 eV, suggesting that their origin may be similar to the multiplet peaks of the 3*p* core level.[20]

The Raman-Auger (constant binding energy) and normal Auger (constant kinetic energy) regions are visible in Fig. 2. The vertical lines are drawn as a guide to the eye to mark the positions of the two Auger peaks. The results of the fitting procedure are given in Fig. 3. The important observations can be summarized as follows: (i) the localized nature of the intermediate state persists up to 1.3±0.2 eV below the absorption threshold, seen as a slope change in the positions of the Auger peaks as a function of incident photon energy, (ii) the measured slope of peak *A* never reaches the value 1 (constant binding energy) before the transition, or 0 (constant kinetic energy) after the transition, (iii) the Auger intensities follow the resonance through the absorption edge with a pro-

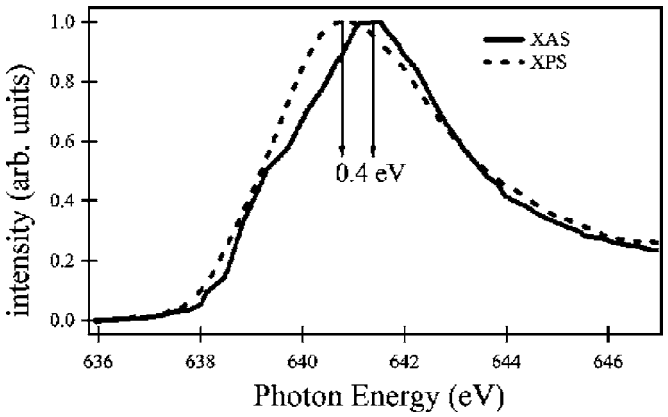

FIG. 4. The absorption spectrum at the L_3 edge of Mn (solid line) is shown along with the $2p$ core level photoemission spectrum (dashed line), plotted as a function of binding energy. The absorption curve was measured by total electron yield.

nounced prepeak feature, and (iv) the $3p$ core level intensity also shows a resonant behavior, which peaks before the Raman-Auger to normal Auger transition.

Leaving the discussion of the first two points to the following sections, we now focus on the photon energy dependence of the intensity of the lower kinetic energy Auger peak *A* shown in Fig. 3. The intensity profile follows the resonant shape of the absorption spectrum, with a clear prepeak around 639.7 eV. At this photon energy, the position of peak *A* is equal, within the uncertainty, to the same Auger feature measured above the L_2 threshold. This coincidence suggests that the prepeak in the intensity profile of the Auger line may be due to an interference between the processes in which the intermediate state is a $2p$ core-hole-excited state with (two-step) or without (one-step) relaxation into the lowest energy XPS core-hole state.[21,22] The relative positions of the absorption and core level photoemission peaks are shown in Fig. 4, where the XPS core-hole state is seen to be at a lower energy by 0.4 eV. This difference means that, within the time before the core-hole decay, the neutral core-hole excited state at resonance will try to relax to the final states of the photoemission process. Indeed, the reduced slope before the normal Auger onset points to the fact that the intermediate state is in part able to relax before the decay takes place. A similar effect is observed between the participant and direct core level contributions to the $3p$ line. The corresponding intensity profile peaks before the Raman to normal Auger transition, settling to a constant value at around the XAS peak (not shown).

Note that the analysis of the energy dispersion has been focussed on the Auger peak labeled as *A*, as the results for peak *B* were rendered unstable due to the overlap with the $3p$ core level peaks in the energy range where the Raman-Auger behavior is observed. Nevertheless, the same transition from Raman-Auger to normal Auger was seen for peak *B* as well, with a considerably reduced slope change compared to that of peak *A*.

IV. RESONANT X-RAY EMISSION RESULTS

Similar to the Auger spectra, we have recorded the Mn $3d2p$ and $3s2p$ RXES spectra as the incident photon energy is tuned through the Mn L_3 edge. The peaks corresponding to the $3d$ to $2p$ emission are shown in Fig. 5(a) for various photon energies. The highest emission energy peak, labeled as *C*, corresponds to the recombination process, whereas at lower energies one can observe the resonant energy-loss features. The two peaks labeled as A' and B', located roughly around 8.5 and 2.5 eV below the recombination peak, are due to excitations within the d-band of Mn.

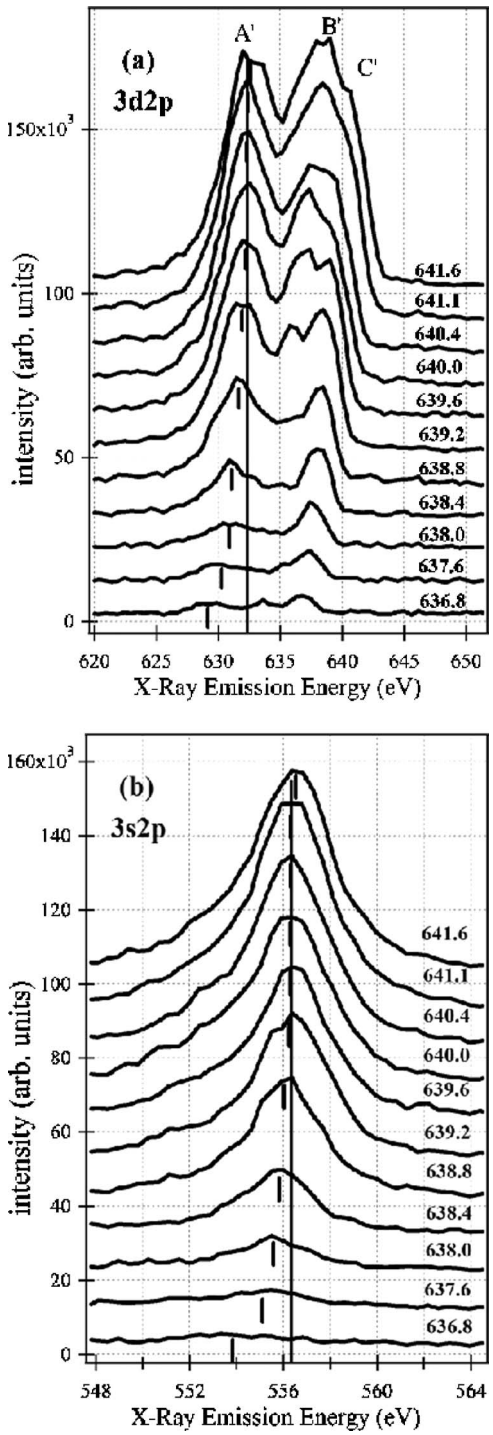

FIG. 5. Mn (a) $3d2p$ ($L\alpha_{1,2}$), (b) $3s2p$ (Ll) RXES spectra as a function of incident photon energy, as noted on the right. For an explanation see the discussion in the text.

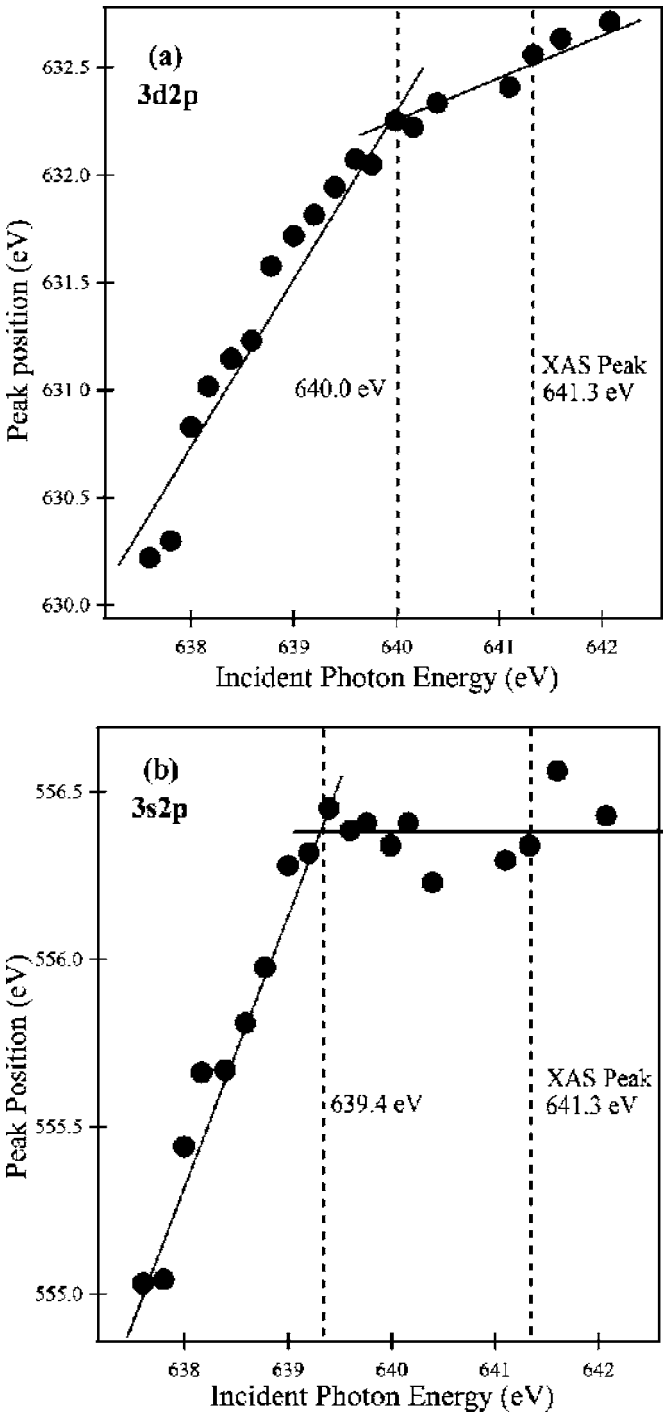

FIG. 6. (a) The position of the $3d2p$ emission peak, labeled as A' in Fig. 5(a) and 5(b) the main peak position for the $3s2p$ emission spectra, as a function of incident photon energy. The transitions from Raman to normal emission are noted on the figures, along with the XAS peak.

The groups of multiplets giving rise to the two features have different amounts of hybridization with the oxygen $2p$ states, and a dominant charge-transfer character is assigned to the lower emission energy peak A'.[23]

In analogy to the Auger emission measurements, the features in the RXES spectra go through a transition as a function of the incident photon energy. This is demonstrated in

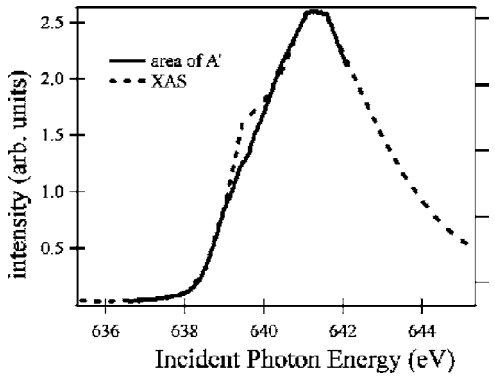

FIG. 7. Intensity of the inelastic scattering peak A' plotted against the incident photon energy, and compared to the x-ray absorption spectrum. See the discussion in the text about the difference observed in the prepeak region.

Fig. 5, where the vertical lines are drawn as a guide to the eye in order to underline the constant emission energy behavior. Especially obvious for A' in $3d2p$ case, the peak position follows the incident photon energy up to the transition after which it stays roughly at constant emission energy. The result of the fit is shown in Fig. 6(a).[24] The slope of the data points before the transition at 640.0 eV is 0.84, corresponding to an almost constant energy loss, whereas after the transition the slope is found to be 0.24, a sign of partially localized nature of the intermediate state persisting above the transition. The photon energy corresponding to the transition is determined to be 1.3 ± 0.2 eV below the absorption threshold.

It is interesting to follow the intensity of the charge-transfer peak A' as a function of the incident photon energy throughout the absorption edge. Seen in Fig. 7, one immediately notices that the prepeak feature in the absorption spectrum is absent in the intensity profile of the emission peak. The explanation is based directly on the coherent nature of the excitation-deexcitation processes. As the prepeak is located before the Raman scattering to normal x-ray emission transition, the ligand (charge transfer) character observed in the final state configuration must be preserved in the intermediate and initial states too. In spite of the numerous multiplet peaks under the XAS spectrum, we can qualitatively group them according to the atomic levels subjected to a crystal field, with the prepeak region corresponding to the empty spin up e_g level assuming 3+ valency with four d electrons. The transition, under the assumption of charge-transfer character throughout the whole process, can be viewed as $3d^4+3d^5L(\text{ground})\rightarrow 2p^5 3d^6L\rightarrow 3d^5L$. The empty e_g level is filled up when a ligand hole L is introduced at the oxygen site, possibly giving an explanation to the missing prepeak in the intensity profile of the charge-transfer feature in the RXES spectra.

The Mn $3s2p$ RXES spectra, seen in Fig. 5(b) were analyzed in the same way as the $3d2p$ peaks. A similar dispersion in the main peak position was observed, with the emission energy increasing linearly with photon energy up to 1.9 ± 0.2 eV below the absorption threshold. The slope was found to be 0.83 before the Raman scattering to normal emission transition, and 0.02 after, suggesting a nearly con-

stant peak position within the uncertainty of the fitting procedure. This dependence of the $3s2p$ peak position on the incident photon energy is shown in Fig. 6(b).

V. DISCUSSION

As was shown for Cr and Fe,[25] and Ni,[26] the Raman to normal Auger transition takes place at or before the ionization threshold (IT), which is obtained from the binding energy of the $2p$ core electron by an XPS measurement. The normal Auger onset at the threshold of a continuum of states was established earlier.[27] An explanation for the observation of normal Auger behavior before the IT was given by a study on V metal, where it was demonstrated that the existence of core-holes in the final state pulls down the $3d$ band.[28] However, for the $La_{0.875}Sr_{0.125}MnO_3$, the $3d$ band is highly localized, and the center of the $4sp$ band is located at considerably higher energies as observed in oxygen K-edge absorption measurements.[29] As a result, any electron exchange contributing to relaxation has to take place by hopping through the states hybridized with the neighboring oxygen atoms. A more pronounced example of this comparison is seen in the case of NiO, with a large bandgap. Interestingly, it was shown that the measured behavior of the various Auger lines through the Ni L_3 resonance can be explained neither by the spectral weight transfer across different multiplets, nor by the distribution of the charge transfer satellites throughout the resonance.[30]

The observation of the Raman scattering on the charge transfer peak A' in Fig. 5(a) is a direct confirmation that having an intermediate state hybridized with the oxygen $2p$ band is not sufficient for relaxation within the core-hole lifetime. This is in spite of the faster hopping times expected from the charge transfer integral, around 2.0 eV,[3] in comparison to the approximate core-hole lifetime width $\sim$0.5 eV. A similar conclusion was reached for NiO through a charge transfer multiplet calculation, with no evidence of a correlation between the weight of the charge transfer states and the normal Auger onset.[30] In the mentioned work, an alternative explanation was sought in the dissipation of the extra energy through low energy excitations such as those involving the creation of phonons. Although it might still be valid for the case of NiO, this effect was shown to be of little significance for CuO, which was confirmed by the absence of a temperature dependence for the Raman to normal Auger transition.[31]

A possible consideration is based on the finite energy resolution of the incident photon beam $\gamma \sim 0.3$ eV. It was demonstrated for broadband excitations ($\gamma > \Gamma$) that one could observe a slope change in the peak positions of the Auger lines as a function of detuning from the center of the resonance.[12,32] Remaining a valid contribution to the measured spectra, this effect should not be significant enough to generate the behavior in the dispersion of the peaks, considering that our photon energy resolution is comparable, but not greater than, the core-hole lifetime width. Moreover, the influence of the spectral resolution would not suffice on its own to explain the final state dependence as summarized in Table I.

TABLE I. The summary of the results of the analysis. The second column is the energy corresponding to the Raman to normal scattering (or Auger emission) transition given in reference to the XAS peak. The third column contains the slope of the peak positions as a function of the incident photon energy after the transition. Note that a zero slope corresponds to constant kinetic energy (emission energy) and a slope of 1 represents constant binding energy (constant energy loss) behavior in the RAES (RXES) process.

Decay Channel	Normal emission onset (eV)	Slope
$2p3p3d$ Auger	L_3-1.3	0.06
$3d2p$ RXES	L_3-1.3	0.24
$3s2p$ RXES	L_3-1.9	0.02

As seen from Table I and Fig. 4, the Raman to normal Auger transition takes place considerably before the IT for all the final states considered, regardless of the absence of a corehole in the final state (RXES $3d2p$). For a more consistent explanation of the measured behavior, we turn our attention to the competition between the relaxation time and the effective scattering duration. As mentioned earlier in the Introduction, the effective duration of the resonant process decreases with increasing detuning Ω. The idea is based on the interference of different states contributing to the scattering, which suppresses the process for times longer than τ_c. It follows that the probability for observing a coherent excitation-deexcitation increases as τ_c decreases, as the system will not have sufficient time for relaxation for scattering faster than the charge transfer times. Through this simplistic model, we obtain the normal Auger onset at an energy Ω_0 before the center of the resonance, according to

$$\tau_{\mathrm{CT}} = \frac{1}{\sqrt{\Omega_0^2 + \Gamma^2}}, \tag{3}$$

where τ_{CT} is the charge transfer time, and Γ is the core-hole lifetime width at resonance. The right hand side of Eq. (3) is actually the asymptotic form of the effective scattering time. A more accurate dependence of this quantity on detuning would require a many-body calculation involving the intermediate state multiplets, which is beyond the scope of this text. However, relying on the formulation above, we obtain $\tau_{\mathrm{CT}} \sim 0.45$ fsec. Note that, in this context, "charge transfer time" stands for "relaxation time" including the possible rearrangement of the $3d$ configurations through inelastic processes as mentioned.

An important point concerns the sign of Ω_0. In principle, we should get a similar dependence of the scattering time both for positive and negative detuning. Note that the assumption, that the intermediate state is discrete, breaks down above the IT, resulting in the normal Auger (or x-ray emission) behavior regardless of the detuning. However, in the case of NiO, the continuum states lie considerably above the resonance. As reported in Ref. 30 the Auger peak positions for NiO indeed go through another slope change after the XAS peak following again a constant binding energy line,

which might be seen as a reemerging Raman process. This may very well be interpreted within the idea as demonstrated in this section.

Lastly, an inspection of the data in Table I results in two observations: (i) the amount of the Raman behavior persisting after the normal Auger onset is reduced by the final state core holes and (ii) an extra electron in the 3*d* levels moves the normal Auger onset to lower energies. The understanding of the first statement can be found in the fact that the 3*d* levels are pulled down in the presence of a core hole in the final state, bringing the continuum states closer to the transition. This explanation is in line with the conclusions from the study on V metal.[28] However, the dependence of the Raman to normal emission transition energy on the final state cannot be explained in the same way. The trend seems to follow the 3*d* electron count in the final state, and according to the model presented in the previous paragraphs, it has to be interpreted as a change in the relaxation time. This point is poorly understood and requires further attention.

VI. CONCLUSION

In this paper we have discussed and compared two different channels of deexcitation (radiative vs radiationless) following the creation of a 2*p* core hole close to the $2p_{3/2}3d$ threshold. These processes differ in the final states reached by the deexcitation, with the RXES having a neutral final state, and the 2*p*3*p*3*d* RAES resulting in a charged state with an additional 3*p* core hole. In the RXES measurements, two different channels corresponding to different final states (with and without a 3*s* core hole) were considered.

From the analysis of the experimental data obtained through these two complementary resonant spectroscopic techniques we have found the following results: (1) the peak corresponding to the charge transfer states in the 3*d*2*p* RXES spectra shows Raman behavior before the resonance, (2) the normal emission behavior is observed at energies considerably lower than the ionization threshold (IT) even for the final state without a core hole, (3) effects related to the incident photon energy resolution are not sufficient to explain the observations. Along these lines, a simple model was developed, in which the Raman to normal emission transition depends on the competition between the relaxation and effective scattering times. From the asymptotic dependence of the scattering time on detuning, an estimate of about 0.45 fs was found for the charge transfer (hopping) time. What still remains to be determined is the contribution of the low-energy excitations to the observed transition, which possibly requires a temperature dependent measurement.

[1] A. J. Millis, Nature (London) **392**, 147 (1998).
[2] M. B. Salamon and M. Jaime, Rev. Mod. Phys. **73**, 583 (2001).
[3] T. Saitoh, A. E. Bocquet, T. Mizokawa, H. Namatame, A. Fujimori, M. Abbate, Y. Takeda, and M. Takano, Phys. Rev. B **51**, 13942 (1995).
[4] Y. Endoh, K. Hirota, S. Ishihara, S. Okamoto, Y. Murakami, A. Nishizawa, T. Fukuda, H. Kimura, H. Nojiri, K. Kaneko, and S. Maekawa, Phys. Rev. Lett. **82**, 4328 (1999).
[5] J. Geck, P. Wochner, S. Kiele, R. Klingeler, P. Reutler, A. Revcolevschi, and B. Büchner, Phys. Rev. Lett. **95**, 236401 (2005).
[6] K. Kuepper, F. Bondino, K. C. Prince, M. Zangrando, M. Zacchigna, A. F. Takács, T. Crainic, M. Matteucci, F. Parmigiani, A. Winiarski, V. R. Galakhov, Ya. M. Mukovskii, and M. Neumann,J. Phys. Chem. B **109**, 15 667 (2005).
[7] A. J. Millis, P. B. Littlewood, and B. I. Shraiman, Phys. Rev. Lett. **74**, 5144 (1995).
[8] P. A. Brühwiler, O. Karis, and N. Martenson, Rev. Mod. Phys. **74**, 703 (2002).
[9] N. Bloembergen, Rev. Mod. Phys. **71**, S283 (1999).
[10] O. Karis, A. Nilsson, M. Weinelt, T. Wiell, C. Puglia, N. Wassdahl, N. Martensson, M. Samant, and J. Stohr, Phys. Rev. Lett. **76**, 1380 (1996).
[11] H. Agren and F. Gel'mukhanov, J. Electron Spectrosc. Relat. Phenom. **110-111**, 153 (2000).
[12] F. Gel'mukhanov and H. Agren, Phys. Rep. **312**, 87 (1999).
[13] M. Zangrando, M. Finazzi, G. Paolucci, G. Comelli, B. Diviacco, R. P. Walker, D. Cocco, and F. Parmigiani, Rev. Sci. Instrum. **72**, 1313 (2001).
[14] D. Cocco, M. Matteucci, K. C. Prince, and M. Zangrando, Proc. SPIE **4506**, 46 (2001).
[15] D. Shulyatev, S. Karabashev, A. Arsenov, and Ya. Mukovskii, J. Cryst. Growth **198/199**, 511 (1999).
[16] R. Zalecki, A. Kolodziejczyk, C. Kapusta, and K. Krop, J. Alloys Compd. **328**, 175 (2001).
[17] M. Richter, P. Bencok, R. Brochier, V. Ilakovac, O. Heckmann, G. Paolucci, A. Goldoni, R. Larciprete, J. -J. Gallet, F. Chevrier, G van der Laan, and K. Hricovini, Phys. Rev. B **63**, 20 5416 (2001).
[18] A. Chainani, M. Mathew, and D. D. Sarma, Phys. Rev. B **47**, 15 397 (1993).
[19] The Auger spectra along with the Mn 3*p* core level were fitted with five Gaussians, chosen as the minimum number of peaks that result in a good fit for all the spectra considered. The background was subtracted as a third order polynomial function. In order to minimize the number of free parameters, the widths of the Gaussians were set to their mean values throughout the incident photon energy range. In spite of the fact that the variation of the peak widths is based on a physical origin, the evaluation of the peak positions was not influenced significantly by the constant width assumption. As an additional constraint, the distance between the two peaks, representing the Mn 3*p* core level, was set to about 1.8 eV. Any asymmetry in the Auger peak shapes was ignored.
[20] B. Hermsmeier, C. S. Fadley, M. O. Krause, J. Jimenez-Mier, P. Gerard, and S. T. Manson, Phys. Rev. Lett. **61**, 2592 (1988).
[21] M. Ohno, Phys. Rev. B **50**, 2566 (1994).
[22] M. Ohno, J. Electron Spectrosc. Relat. Phenom. **148**, 41 (2005).
[23] K. Kuepper, M. C. Falub, K. C. Prince, V. R. Galakhov, I. O. Troyanchuk, S. G. Chiuzbaian, M. Matteucci, D. Wett, R. Szargan, N. A. Ovechkina, Ya. M. Mukovskii, and M. Neu-

mannJ. Phys. Chem. B **109**, 9354 (2005).

[24] In the RXES $3d2p$ spectra, three peaks were used to fit the charge transfer, *d-d* excitation and recombination features. The recombination peak was fitted with a Gaussian, whereas a convolution of a Gaussian with a Lorentzian was used for the other two components. In a similar fashion to the RAES spectra, any asymmetry of the peak shapes or variation of the peak widths was ignored. The $3s2p$ spectra were fitted with two peaks with a separation of approximately 3.5 eV. All the RXES spectra were normalized by the integrated intensity of the oxygen $2p1s$ emission.

[25] S. Hüfner, S.-H. Yang, B. S. Mun, C. S. Fadley, J. Schäfer, E. Rotenberg, and S. D. Kevan, Phys. Rev. B **61**, 12582 (2000).

[26] M. Weinelt, A. Nilsson, M. Magnuson, T. Wiell, N. Wassdahl, O. Karis, A. Föhlisch, N. Martensson, J. Stöhr, and M. Samant, Phys. Rev. Lett. **78**, 967 (1997).

[27] T. Aberg and B. Crasemann, *Resonant Anomalous X-Ray Scattering* (Elsevier, Amsterdam, 1994), p. 431.

[28] V. Ilakovac, M. Kralj, P. Pervan, M. C. Richter, A. Goldoni, R. Larciprete, L. Petaccia, and K. Hricovini, Phys. Rev. B **71**, 085413 (2005).

[29] M. Abbate, F. M. F. de Groot, J. C. Fuggle, A. Fujimori, O. Strebel, F. Lopez, M. Domke, G. Kaindl, G. A. Sawatzky, M. Takano, Y. Takeda, H. Eisaki, and S. Uchida, Phys. Rev. B **46**, 4511 (1992).

[30] M. Finazzi, N. B. Brookes, and F. M. F. de Groot, Phys. Rev. B **59**, 9933 (1999).

[31] M.Finazzi, G. Ghiringhelli, O. Tjernberg, P. Ohresser, and N. B. Brookes, Phys. Rev. B **61**, 4629 (2000).

[32] E. Kukk, S. Aksela, and H. Aksela, Phys. Rev. A **53**, 3271 (1996).